

Structure of Langmuir films by second-harmonic reflection

O. A. Aktsipetrov, N. N. Akhmediev, I. M. Baranova, E. D. Mishina, and V. R. Novak

M. V. Lomonosov State University, Moscow

(Submitted 25 December 1984)

Zh. Eksp. Teor. Fiz. **89**, 911–921 (September 1985)

A nonlinear optical method for analyzing the structure of submono-, mono-, and multilayer Langmuir films is developed which exploits the generation¹ of reflected second harmonics. The method is used to determine the mutual orientation of neighboring monolayers in multilayer Langmuir films, find the preferred orientation of the microcrystallites, and analyze the molecular alignment in the film. Multilayer noncentrosymmetric films with large quadratic susceptibilities are also grown which are well-suited for high-efficiency optoelectronic frequency converters.

1. INTRODUCTION

Second-harmonic generation (SHG) accompanying the reflection of laser light by monomolecular Langmuir films was discovered in Ref. 1 and should permit the design of optoelectronic frequency converters from such films. As in other types of optoelectronic devices,^{2,3} efficient frequency conversion requires that the Langmuir films have precisely specified structural properties. For second-harmonic Langmuir converters the packing of the layers in the films must be noncentrosymmetric. However, since x-ray structure methods are seldom applicable to films containing only a few layers, other techniques are needed. Nonlinear optical methods have recently attracted much interest in solid-state surface studies. For example, giant Raman scattering⁴ and nonlinear optical electron reflection accompanying giant SHG (Ref. 5) yield information about molecular adsorption on metal surfaces⁶ and can be used to measure the zero charge potentials.⁷ The reflected second-harmonic method has been used to study laser annealing,⁸ molecular adsorption on semiconductor surfaces,⁹ and the crystal structure of surface layers in single crystals.¹⁰

The purpose of our present work was to develop a nonlinear optical method for analyzing the structure of Langmuir films and to grow multilayer films with large nonlinear susceptibilities.

2. NONLINEAR OPTICAL METHOD OF STRUCTURE ANALYSIS AND TECHNIQUE FOR GROWING LANGMUIR FILMS

We analyzed the structure of NAB (4-nitro-4'-octadecylazobenzene) films by recording the intensity $I_{2\omega}$ of the reflected second harmonic as a function of the rotation angle φ of the film relative to an axis normal to the film surface (the rotation axis passed through the plane of incidence and the center of the pumping radiation spot). We used both *p*- and *s*-polarized pumping beams and studied the intensity of the *s*- and *p*-polarized second-harmonic radiation. For multilayer films we measured $I_{2\omega}$ as a function of the number of layers *N*, while for submonolayer films we studied how the intensity varied with the concentration of NAB molecules in a cadmium arachinoate-arachinoic acid matrix.

We observed SHG when radiation pulses from a *Q*-switched YAG: Nd³⁺ laser were reflected by the Langmuir films; the laser wavelength was $\lambda = 1060$ nm, the pulses

were $\tau \sim 20$ ns long, and the energy per pulse was $W \sim 0.5$ – 5 mJ. The pumping beam made a constant angle of 45° with the normal to the film, which was rotated about an axis which was normal to the film and passed exactly through the center of the pumping radiation spot. The spot radius was varied from ~ 0.1 to 5 mm by moving the lens used to focus the pumping radiation. The second harmonic radiation at $\lambda = 532$ nm was focused by a lens system onto the entrance slit of a DFS-24 monochromator. The SH intensity at the output of the monochromator was recorded by an FÉU-79 photomultiplier and a high-speed strobed *A/D* converter. The recording system was calibrated in terms of the SH intensity reflected from a silver surface, for which the SH conversion factor is known¹¹: $r = (cI_{2\omega}/8\pi I_{\omega}^2)^{1/2} = 1.3 \cdot 10^{-9}$ (cgse units), where I_{ω} is the pump intensity.

The monomolecular Langmuir layers were first grown on a water surface from a solution of NAB in benzene, after which the monolayer was transferred to a fused quartz substrate at a constant surface pressure. The submonomolecular layers consisted of a mixture of NAB and arachinoic acid and were transferred during growth by pulling the substrate across the interface while simultaneously compressing the region of the water surface containing the monolayer film. The surface density of molecules in the monolayer was calculated from the transport coefficient and found to be $N_{\eta} \sim 3 \cdot 10^{14}$ cm⁻². For the mono- and multilayer NAB films, each subsequent monolayer was transferred by dipping the hydrophobic substrate through the water surface on which a NAB monolayer was floating; the substrate was then drawn across a pure water interface uncoated by film.¹² Multilayer Langmuir films with noncentrosymmetric layer packing were grown by repeating the dipping-drawing cycle. During formation on the water surface, the monolayer was compressed along the direction of motion of the edge of the meniscus as the substrate crossed the interface.

3. THEORY OF ANISOTROPIC SECOND HARMONIC GENERATION DURING REFLECTION OF LIGHT BY LANGMUIR FILMS

Bloembergen and Pershan¹³ first considered the theory of SHG by a nonlinear plate. We supplement their results here by examining layers with a highly anisotropic nonlinearity and allowing for the nonlinear polarization wave generated when the pumping radiation is reflected by the bot-

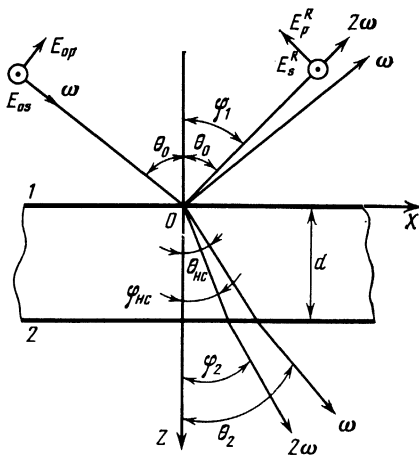


FIG. 1. Experimental geometry for recording second-harmonic generation accompanying reflection from a Langmuir film: the linear media 1, 2 in $z < 0$ and $z > d$ have dielectric permittivities ϵ_1, ϵ_2 ; the nonlinear Langmuir film occupies the region $0 < z < d$; θ_0, θ_1 , and θ_2 are the angles between the normal to the film and the wave vectors of the pumping light in medium 1, in the film, and in medium 2, respectively; φ_0, φ_1 , and φ_2 are the corresponding angles for the second-harmonic radiation; E_{0p} and E_{0s} are the polarizations of the pumping light, and E_s^R, E_p^R are the polarizations of the SH light.

tom edge of the film. We also treat the anisotropy of the linear dielectric permittivity.

We thus consider two linear semiinfinite media 1, 2 with permittivities ϵ_1, ϵ_2 (Fig. 1) bounding a thin uniform nonlinear layer of thickness $d \ll \lambda$ with a quadratic susceptibility χ and a linear permittivity tensor described by its three principal components $\epsilon_x(\omega), \epsilon_y(\omega), \epsilon_z(\omega)$. The $Z = 0$ plane coincides with the interface between medium 1 and the nonlinear film, and the Z axis points normal to the film into medium 2. Pumping radiation $E(\omega)$ with amplitude E_0 is incident on medium 1 at an angle θ_0 to the Z axis. It is difficult to derive reasonably simple expressions for the dependence of the reflected SH field on the nonlinear polarization for arbitrary orientations of the incident plane relative to the principal X, Y axes. However, if one of the axes (say X) lies in the plane of incidence, we can derive the expressions

$$E^p(2\omega) = -\frac{i8\pi\omega c^{-1}d \cos \varphi_2}{\epsilon_2^{1/2}(2\omega) \cos \varphi_1 + \epsilon_1^{1/2}(2\omega) \cos \varphi_2} \times \left(\frac{\epsilon_2(2\omega)}{\epsilon_z(2\omega)} \operatorname{tg} \varphi_2 P_z^N + P_x^N \right), \quad (1)$$

$$E^s(2\omega) = \frac{i8\pi\omega c^{-1}d P_y^N}{\epsilon_2^{1/2}(2\omega) \cos \varphi_2 + \epsilon_1^{1/2}(2\omega) \cos \varphi_1}, \quad (2)$$

for the field amplitudes of the reflected p - and s -polarized second-harmonic waves under our assumptions. Here φ_1 and φ_2 are the angles between the Z axis and the SH wave vectors in media 1 and 2, respectively. We note that in the present case all components of the linear dielectric tensor vanish, except for ϵ_z in expression (1) for the p -polarized SH radiation. For a uniaxial crystal with optic axis normal to the film, Eqs. (1) and (2) are valid for all orientations of the plane of incidence relative to the X, Y axes. We note that all Langmuir films known to date are optically uniaxial with optic axis normal to the plane of the film.

For p -polarized pumping radiation the components of the nonlinear polarization in the nonlinear film are related to the components of the pumping radiation field by

$$P_x^N = \chi_{xxx} E_x^2(\omega) + 2\chi_{xxz} E_x(\omega) E_z(\omega) + \chi_{xzz} E_z^2(\omega), \quad (3)$$

$$P_y^N = \chi_{yyx} E_x^2(\omega) + 2\chi_{yyz} E_x(\omega) E_z(\omega) + \chi_{yzz} E_z^2(\omega), \quad (4)$$

$$P_z^N = \chi_{zzx} E_x^2(\omega) + 2\chi_{zzz} E_x(\omega) E_z(\omega) + \chi_{zzz} E_z^2(\omega). \quad (5)$$

The field components at the fundamental frequency inside the film are given by

$$E_x(\omega) = k_z [C \exp(ik_z z) - D \exp(-ik_z z)] (k_0 \epsilon_x(\omega))^{-1}, \\ E_z(\omega) = -k_x [C \exp(ik_z z) + D \exp(-ik_z z)] (k_0 \epsilon_z(\omega))^{-1}, \quad (6)$$

where k_z and k_x are the components of the wave vector of the pumping radiation in the film and $k_0 = \omega/c$, where c is the velocity of light in vacuum. Expressions for the coefficients C and D can be derived from the boundary conditions for the tangential components of the electric and magnetic field. In the limit $d \rightarrow 0$, the components of the pumping field in the nonlinear film are related to the field in medium 1 by

$$E_x(\omega) = \frac{2\epsilon_1^{1/2}(\omega) \cos \theta_2 \cos \theta_0}{\epsilon_1^{1/2}(\omega) \cos \theta_2 + \epsilon_2^{1/2}(\omega) \cos \theta_0} E_{0x}, \\ E_z(\omega) = -\frac{\epsilon_2(\omega)}{\epsilon_z(\omega)} \operatorname{tg} \theta_2 E_x(\omega), \quad (7)$$

where θ_2 is the angle between the Z axis and the pump wave vector in medium 2. If we substitute (7) into (3) and (5) and insert the resulting expressions for the nonlinear polarization components into (1), we get the expression

$$\frac{E^{p,p}(2\omega)}{E_0^2} = -\frac{i8\pi\omega c^{-1}d \cos \varphi_2}{\epsilon_2^{1/2}(2\omega) \cos \varphi_1 + \epsilon_1^{1/2}(2\omega) \cos \varphi_2} \times \left(\frac{2\epsilon_1^{1/2}(\omega) \cos \theta_2 \cos \theta_0}{\epsilon_1^{1/2}(\omega) \cos \theta_2 + \epsilon_2^{1/2}(\omega) \cos \theta_0} \right)^2 \chi_{eff}^{p,p} \quad (8)$$

for the p -polarized component of the reflected SH field for a p -polarized pump, where

$$\chi_{eff}^{p,p} = \chi_{zzz} \alpha^2 \beta - 2\chi_{zzx} \beta \alpha + \chi_{xxx} \beta - \chi_{xxx} - 2\chi_{xxz} \alpha + \chi_{xzz} \alpha^2, \quad (9)$$

$$\beta = \frac{\epsilon_2(2\omega)}{\epsilon_z(2\omega)} \operatorname{tg} \varphi_2, \quad \alpha = \frac{\epsilon_2(\omega)}{\epsilon_z(\omega)} \operatorname{tg} \theta_2. \quad (10)$$

Similarly, substitution of (7) into (4) and insertion of the resulting relation for P_y^N into (2) yield

$$\frac{E^{s,p}(2\omega)}{E_0^2} = \frac{i8\pi\omega c^{-1}d}{\epsilon_2^{1/2}(2\omega) \cos \varphi_2 + \epsilon_1^{1/2}(2\omega) \cos \varphi_1} \times \left(\frac{2\epsilon_1^{1/2}(\omega) \cos \theta_2 \cos \theta_0}{\epsilon_1^{1/2}(\omega) \cos \theta_2 + \epsilon_2^{1/2}(\omega) \cos \theta_0} \right)^2 \chi_{eff}^{s,p}, \quad (11)$$

$$\chi_{eff}^{s,p} = \chi_{yzz} \alpha^2 - 2\chi_{yyz} \alpha + \chi_{yyx} \quad (12)$$

for the s -polarized component of the reflected SH field for a p -polarized pump.

The same procedure can be used to find the amplitudes of the p - and s -polarized components of the reflected SH field for an s -polarized pump:

$$\frac{E^{p,s}(2\omega)}{E_0^2} = -\frac{i8\pi\omega c^{-1}d \cos \varphi_2}{\epsilon_2^{1/2}(2\omega) \cos \varphi_1 + \epsilon_1^{1/2}(2\omega) \cos \varphi_2} \times \left(\frac{2\epsilon_1^{1/2}(\omega) \cos \theta_0}{\epsilon_1^{1/2}(\omega) \cos \theta_0 + \epsilon_2^{1/2}(\omega) \cos \theta_2} \right)^2 \chi_{eff}^{p,s}, \quad (13)$$

where

$$\chi_{eff}^{p,s} = \beta \chi_{xyy} + \chi_{xyy}; \quad (14)$$

$$\frac{E^{s,s}(2\omega)}{E_0^2} = \frac{i8\pi\omega c^{-1}d}{\varepsilon_2^{1/2}(2\omega) \cos \varphi_2 + \varepsilon_1^{1/2}(2\omega) \cos \varphi_1} \times \left(\frac{2\varepsilon_1^{1/2}(\omega) \cos \theta_0}{\varepsilon_1^{1/2}(\omega) \cos \theta_0 + \varepsilon_2^{1/2}(\omega) \cos \theta_2} \right)^2 \chi_{eff}^{s,s}, \quad (15)$$

where

$$\chi_{eff}^{s,s} = \chi_{yyy}. \quad (16)$$

We will next derive an expression for the effective susceptibilities χ_{eff} in terms of φ for a uniaxial crystal with optic axis normal to the film (φ is the rotation angle of the nonlinear film about the Z axis). We denote the rotating coordinate system associated with the film by X', Y', Z' , while the (stationary) laboratory frame in which the SH intensity is measured is denoted by X, Y, Z . We assume that the two coordinate systems coincide initially, after which we rotate the film by φ about the Z (Z') axis. The components χ_{ijk} and χ'_{ijk} of the quadratic susceptibility tensor in the lab and film frames are related as usual by

$$\chi_{ijk} = a_{in}' a_{jl}' a_{km}' \chi'_{ilm}, \quad a_{ij}' = \begin{pmatrix} \cos \varphi & -\sin \varphi & 0 \\ \sin \varphi & \cos \varphi & 0 \\ 0 & 0 & 1 \end{pmatrix}. \quad (17)$$

If we use (17) to express χ_{ijk} in (9) in terms of χ'_{ijk} and a'_{ij} , we get the result

$$\chi_{eff}^{p,p} = A_0^{p,p} + A_1 \sin \varphi + A_2 \sin 2\varphi + A_3 \sin 3\varphi + B_1 \cos \varphi + B_2 \cos 2\varphi + B_3 \cos 3\varphi \quad (18)$$

for $\chi_{eff}^{p,p}$ as a function of the rotation angle φ .

Similar expressions with different coefficients A_i, B_i hold for the effective susceptibilities $\chi_{eff}^{s,p}, \chi_{eff}^{p,s}, \chi_{eff}^{s,s}$. Only four of the terms are nonzero for $\chi_{eff}^{s,s} - A_0^{s,s} = A_2^{s,s} = B_2^{s,s} = 0$. Table I gives the expressions for the coefficients A_i, B_i . We see that in general, the $\chi_{eff}(\varphi)$ are expressible as Fourier series in which only the first seven terms are nonzero. If experimental data are available for $\chi_{eff}(\varphi)$ one can then calculate the coefficients A_i, B_i , which are linear combinations of the tensor components χ'_{ijk} . In general, the tensor χ has 18 independent components for a nonlinear film of arbitrary symmetry. Each of the three dependences $\chi_{eff}^{p,p}(\varphi), \chi_{eff}^{s,p}(\varphi)$, and $\chi_{eff}^{p,s}(\varphi)$, gives seven equations for determining the χ'_{ijk} , while $\chi_{eff}^{s,s}$ yields four equations. We thus have 25 equations altogether for the 18 unknown components of χ , and if the expansion coefficients A_i, B_i are known accurately enough [this depends on the error in measuring the $\chi_{eff}(\varphi)$ and on how uniform the film is], the components χ'_{ijk} can in principle be calculated for homogeneous films.

We note that the angular dependence $I_{2\omega}(\varphi)$ of the second-harmonic intensity can be measured experimentally and is proportional to $[\chi_{eff}(\varphi)]^2$. The Fourier spectrum for $\chi_{eff}(\varphi)$ can then be uniquely reconstructed if $[\chi_{eff}(\varphi)]^2$ does not vanish for any φ between 0 and 2π , as was the case in our experiments.

4. EXPERIMENTAL STUDIES OF THE STRUCTURE OF MONO- AND MULTILAYER LANGMUIR FILMS

We studied the structure of the films by recording the angular dependence $I_{2\omega}(\varphi)$ of the second-harmonic intensity for films with from 1 to 6 NAB monolayers.

The dependence of the angle-averaged intensity $\langle I_{2\omega} \rangle$ on the number of monolayers N can be used to determine if the layer packing is centrally symmetric or not. Figure 2 plots the quantity

$$r = \left[\frac{c}{8\pi} \langle I_{2\omega} \rangle I_{\omega}^{-2} \right]^{1/2}$$

as a function of N . The linear dependence indicates that the packing was noncentrosymmetric, in good agreement with the previously observed pyroelectric effect in multilayer NAB films and with the results of x-ray structure measurements¹⁴ (the monolayer period along the Z axis is equal to 26.3 Å).

We recorded $I_{2\omega}(\varphi)$ for both mono- and multilayer Langmuir films illuminated by p -polarized pumping light. The angle φ was chosen to be equal to zero when the film was oriented so that the meniscus (compressed region) moved along the X axis in the plane of incidence. The measurements were made for various samples by focusing the laser light at different points. Two types of angular dependences were found. The first, more common type (observed in more than 60% of the cases) had a pronounced peak either at $\varphi \sim 90^\circ$ or at $\varphi \sim 270^\circ$ (Figs. 3, 4). Such behavior is typical for both mono- and multilayer films. The second type was smoother and had weaker maxima which did not occur at any particular angle φ (Fig. 5).

Infrared spectral studies, electron diffraction, and electron microscopy have shown that even the simplest Langmuir films (such as those consisting of carbonic acids and their salts) consist of crystallites belonging to the less symmetric triclinic and monoclinic crystal classes.¹⁵ Depending on the type of film, the microcrystallite diameters may vary widely from a few tenths of a micrometer to a fraction of a millimeter (as, for example, in diacetylene films¹⁶). In most Langmuir films the microcrystallites are isotropically distributed in the plane of the film; however, in a few cases there is a preferred orientation in the film plane which is determined by how the monolayers are laid down.^{17,18} On the other hand, optical measurements reveal that Langmuir films are uniaxial crystals with optic axis normal to the plane of the film.^{19,20} No observations or measurements of in-plane refractive index anisotropy have been reported for Langmuir films. We note that even the linear dielectric permittivity in Langmuir films is nearly isotropic in and normal to the film plane, $(\varepsilon_z - \varepsilon_x)/\varepsilon_z = 0.06$ (Ref. 20). Whatever anisotropy is present is due to the fact that the films are composed of nearly vertical rod-shaped molecules.

Since our films also consisted of rod-shaped molecules, there is no reason to expect the linear dielectric permittivity to be significantly anisotropic in the plane of the film. We further observe that the nonlinearity of the NAB molecule is due to its long chain of conjugated atoms, which contains donor and acceptor groups at opposite ends. In molecules of this type, the axial component of the molecular hyperpolariz-

TABLE I. Fourier expansion coefficients A_i, B_i for the reflected second-harmonic field for various pump and SH signal polarizations ($k = p, s; l = p, s$).

	p, p	s, p	s, s	p, s
$A_0^{k,l}$	$\alpha^2\beta\chi'_{zzz} + \beta\chi'_{zzx} - \alpha\chi'_{zzx} + \beta\chi'_{zyy} - \alpha\chi'_{zyz}$	$1/2\alpha(\chi'_{xyz} - \chi'_{yxz})$	0	$1/2\beta(\chi'_{zyy} + \chi'_{zzx})$
$A_1^{k,l}$	$-\alpha^2\chi'_{jzz} + 2\alpha\beta\chi'_{zzy} - 1/4(3\chi'_{yyy} + 2\chi'_{xxy} + \chi'_{yxx})$	$\alpha^2\chi'_{zzz} + 1/8(3\chi'_{xyy} - 2\chi'_{yyx} + \chi'_{xxx})$	$1/4(3\chi'_{xxx} + 2\chi'_{yyx} + \chi'_{xyy})$	$1/4(\chi'_{xyx} + \chi'_{xxy} - \chi'_{yyy} - 3\chi'_{yxx})$
$A_2^{k,l}$	$-\beta(\chi'_{xxy} + \chi'_{zyx}) + \alpha(\chi'_{xyz} + \chi'_{yxz})$	$1/2\alpha(\chi'_{jyz} - \chi'_{xxx})$	0	$1/2\beta(\chi'_{zjx} + \chi'_{zxy})$
$A_3^{k,l}$	$1/4(\chi'_{yyy} - 2\chi'_{xxy} - \chi'_{yxx})$	$1/2(\chi'_{xxx} - 2\chi'_{yyx} - \chi'_{xyy})$	$-1/4(\chi'_{xxx} - 2\chi'_{yyx} - \chi'_{xyy})$	$1/4(\chi'_{xyx} + \chi'_{xxy} - \chi'_{yyy} + \chi'_{jxx})$
$B_1^{k,l}$	$\alpha^2\chi'_{zzz} - 2\alpha\beta\chi'_{zzx} + 1/4(3\chi'_{xxx} + 2\chi'_{jyx} + \chi'_{xyy})$	$-\alpha^2\chi'_{jzz} - 1/8(3\chi'_{yxx} - 2\chi'_{xxy} + \chi'_{yyy})$	$1/4(3\chi'_{yyy} + 2\chi'_{xxy} + \chi'_{jxx})$	$1/4(3\chi'_{xyy} + \chi'_{xxx} - \chi'_{jyx} - \chi'_{yxy})$
$B_2^{k,l}$	$\beta(\chi'_{zzx} - \chi'_{zyy}) + \alpha(\chi'_{jyz} - \chi'_{xxx})$	$-1/2\alpha(\chi'_{jzz} + \chi'_{xyz})$	0	$1/2\beta(\chi'_{zjy} - \chi'_{zxx})$
$B_3^{k,l}$	$1/4(\chi'_{xxx} - 2\chi'_{jyx} - \chi'_{xyy})$	$1/8(\chi'_{yxx} - \chi'_{yyy} + 2\chi'_{xxy})$	$1/8(\chi'_{yyy} - 2\chi'_{xxy} - \chi'_{jxx})$	$1/8(\chi'_{xyy} - \chi'_{xxx} + \chi'_{jyx} + \chi'_{yxy})$

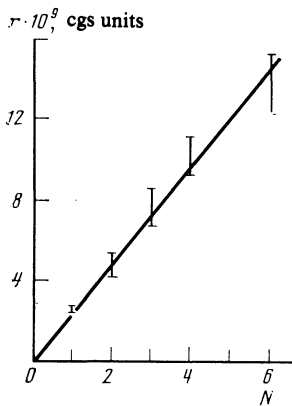


FIG. 2. Conversion factor $r = [(c/8\pi) \langle I_{2\omega} \rangle I_{\omega}^{-2}]^{1/2}$ versus number N of NAB monolayers in multilayer Langmuir films. The linear dependence shows that $I_{2\omega}$ increases quadratically with N .

zability is many times greater than the other components, whereas the anisotropy of the linear polarizability is considerably less pronounced.²¹ Moreover, if these molecules have a preferred orientation then any mismatch θ from this direction will have a greater influence on the decrease in the anisotropy of the linear permittivity, because the longitudinal component gives contributions $\sim \langle \cos^2 \theta \rangle$ and $\sim \langle \sin^2 \theta \rangle$ to the linear permittivity along and normal to the preferred direction, respectively, while these contributions are $\sim \langle \cos^3 \theta \rangle$ and $\sim \langle \sin^3 \theta \rangle$ for the nonlinear susceptibility.

The behavior of the curves $I_{2\omega}(\varphi)$ leads to the following conclusions regarding the structure of our NAB films. The films are nonuniform and consist of microcrystallites of various orientations. There exist regions of diameter ~ 0.5 mm comparable to the size of the illuminated spot in which the microcrystallites have a preferred inplane orientation normal to the X axis, i.e., to the direction of motion of the meniscus (compressed region). On the other hand, in other regions the microcrystallites have a preferred orientation along or antiparallel to the X axis [this corresponds to maxima at $\varphi \sim 90^\circ$ and $\varphi \sim 270^\circ$, respectively (Figs. 3 and 4)]. Finally, in some regions the crystallites are randomly oriented, and in this case the angular dependences are smoothed out and have peaks at random values of φ (Fig. 5). Similarly,

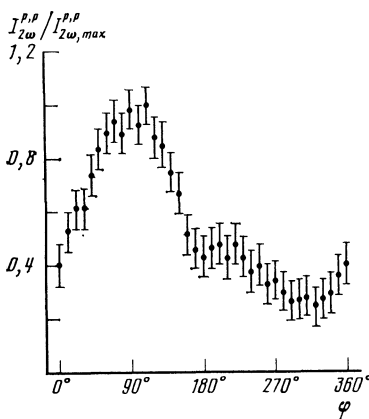


FIG. 3. Second-harmonic intensity versus angle φ for monolayer NAB films. The preferred orientation of the microcrystallites is along the direction $\varphi = 90^\circ$; the illuminated spot was ~ 0.5 mm in diameter.

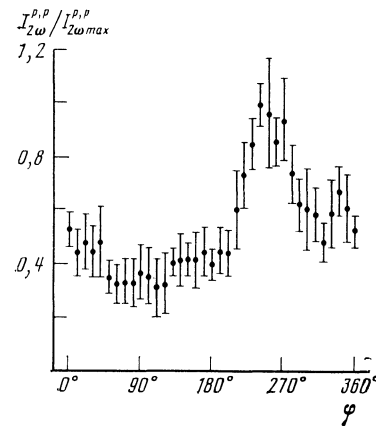


FIG. 4. Second-harmonic intensity as a function of φ for a film with $N = 4$ monolayers. The spot diameter was ~ 0.5 mm, and the preferred microcrystallite orientation is along the direction $\varphi = 270^\circ$.

as the illuminated spot becomes larger the angular averaging extends over a larger region, which also tends to smooth out the curves.

If we assume that the linear permittivity in the film plane is perfectly isotropic, we can express the effective susceptibility in the form

$$\chi_{eff}^{p,p} = \chi_0^{p,p} (1 + \alpha_1 \sin \varphi)$$

for the angular dependences shown in Figs. 3 and 4. The parameter α_1 is determined by the Fourier expansion of $[I_{2\omega}(\varphi)]^{1/2}$ in terms of φ and lies in the range $\alpha_1 = \pm (0.12-0.3)$. The measurement error was too large to permit us to calculate the higher-order terms in the Fourier expansion. The susceptibility $\chi_0^{p,p}$ for NAB Langmuir films calculated from (8) is $\chi_0^{p,p} = (3.7 \pm 0.5) \cdot 10^8$ (cgs units). We have thus shown that the quadratic nonlinear susceptibility in noncentrosymmetric multilayer NAB Langmuir films is comparable to the susceptibility for lithium niobate crystals.

5. EXPERIMENTAL STUDY OF THE STRUCTURE OF SUBMICRON FILMS

The nonlinear optical technique is sensitive enough to record the SH signal even for submonolayer NAB films, in

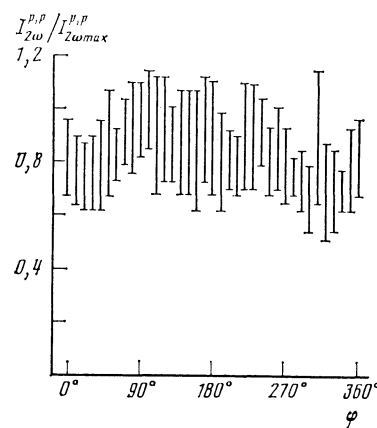


FIG. 5. Second-harmonic intensity versus φ for a film with $N = 6$ monolayers. The dependence is isotropic without sharp peaks (spot diameter ~ 2 mm).

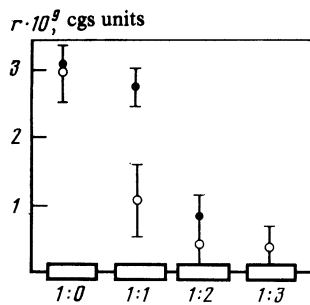


FIG. 6. Conversion factor $r = [(c/8\pi)\langle I_{2\omega} \rangle I_{\omega}^{-2}]^{1/2}$ for a submonolayer film as a function of the relative concentration C of NAB molecules in a cadmium arachinoate matrix for s - and p -polarized pumping and SH light. ●, p -polarized pump and SH signal; ○, s -polarized pump and SH signal.

which the NAB molecules lie in a matrix of surface-active molecules with a small quadratic hyperpolarizability (e.g., a mixture of cadmium arachinoate and arachinoic acid). The structure and nonlinear optical properties are quite different for submonolayer films.

Figure 6 shows how r depends on the NAB concentration C in the matrix for the p - and s -polarized SH components for p - and s -polarized pumping light, respectively. We write $1:n$ to indicate that n molecules of cadmium arachinoate-arachinoic acid are present for each NAB molecule. We first note that for a monolayer NAB film ($1:0$), the strong s -component of the SH signal for s -polarized pumping light indicates that the film lacks C_{∞} symmetry about the Z axis, since otherwise the s -component of the SH signal would vanish for an s -polarized pump. As C decreases, the behavior of r differs for p - and s -polarized SH light. The p -component for a p -polarized pump drops nearly fourfold when C decreases from $1:1$ to $1:2$, while the s -polarized component of the SH signal for an s -polarized pump drops by a factor of ~ 15 . This indicates that the submonolayer Langmuir film takes on the C_{∞} symmetry as C decreases. We attribute this partly to a change in the NAB molecule orientation with respect to the Z axis, and partly to misorientation of the molecules in the film plane (possibly without any change in orientation relative to the Z axis). We have already noted that the NAB molecule contains a long conjugated chain with donor and acceptor groups at either end. For this molecular structure, the $\gamma_{z''z''z''}$ component of the quadratic hyper-polarizability tensor should be the dominant component (the Z'' axis of the molecular coordinate system points along the donor-acceptor chain).

In view of the results in the previous section, we can qualitatively explain the findings for submonolayer NAB films by considering a crude model, according to which the NAB molecules in a monolayer Langmuir film are aligned so that their Z'' axes point in some preferred direction, which we take to lie in the YZ plane, and make an angle ψ with the Z axis. The s - or p -polarized pumping light will then cause the components P_y (respectively, P_z) of the nonlinear macroscopic polarization to be nonzero; these components are responsible for generating the s - and p -polarized SH signals, respectively. According to Ref. 22, the polarization components are given by

$$P_y \sim N_n \gamma_{z''z''z''} \langle \sin^3 \psi \rangle E_0^2, \quad P_z \sim N_n \gamma_{z''z''z''} \langle \cos^3 \psi \rangle E_0^2, \quad (19)$$

where N_n is the surface density of the NAB molecules.

The average angle between the Z and molecular axes does not change significantly as C decreases— this follows from expression (19) for P_z and the fact that a threefold drop in C causes $I_{2\omega}^{1/2}$ for the p -polarized SH signal to decrease by a factor of ~ 4 . In order to explain the large drop in the P_y component, we must thus assume that the molecules become misoriented in the plane of the film as C decreases. Using (19) and (1), (2), we find the rough estimate $\sim 30^\circ$ for the average inclination angle of the NAB molecules in a monolayer; this compares with the value $\sim 46^\circ$ for multilayer NAB Langmuir films found from x-ray structure analysis¹⁴ and the known length of the molecule.

6. CONCLUSIONS

Our analysis shows that nonlinear optical techniques are well-suited for studying the properties and structure of submono-, mono-, and multilayer Langmuir films. Specifically, measurements of second-harmonic generation accompanying the reflection of light by Langmuir films can be used to find the quadratic susceptibility the mutual orientation of neighboring monolayers in a multilayer film, the preferred microcrystallite orientations, and the molecular alignment inside the film.

Our results are the first to be reported for noncentrosymmetric multilayer Langmuir films with a large quadratic susceptibility. We measured the effective quadratic susceptibility of NAB films, which was found to be comparable to the susceptibility of lithium niobate crystals.

Our analysis indicates that NAB Langmuir films are polycrystalline with a nonuniform crystallite orientation. However, in certain regions of the film the microcrystallites are preferentially oriented normal to the direction of motion of the meniscus in the plane of the film. The nonlinear optical properties of submonolayer NAB films are much more nearly isotropic, probably because the spatial distribution in the film plane is more uniform.

We close by thanking L. V. Keldysh for suggesting this topic of study and for helpful discussions, and V. T. Lazarev for synthesizing the NAB.

¹O. A. Aktsipetrov, N. N. Akhmediev, E. D. Mishina, and V. R. Novak, *Pis'ma Zh. Eksp. Teor. Fiz.* **37**, 175 (1983) [*JETP Lett.* **37**, 207 (1983)].

²L. M. Blinov, *Usp. Khim.* **52**, 1263 (1983).

³*Thin Solid Films* **99**, 1-327 (1983).

⁴*Giant Raman Scattering* [Russian translation edited by V. M. Agronovich], Mir, Moscow (1984).

⁵O. A. Aktsipetrov, E. D. Mishina, and A. V. Petukhov, *Pis'ma Zh. Eksp. Teor. Fiz.* **38**, 442 (1983) [*JETP Lett.* **38**, 535 (1983)].

⁶C. K. Chen, T. F. Heinz, D. Ricard, and Y. R. Shen, *Chem. Phys. Lett.* **83**, 455 (1981).

⁷O. A. Aktsipetrov, V. Ya. Bartenev, E. D. Mishina, and A. V. Petukhov, *Kvantovaya Elektron. (Moscow)* **10**, 1113 (1983) [*Sov. J. Quantum Electron.* **13**, 712 (1983)].

⁸S. A. Akhmanov, S. A. Galyautdinov, N. I. Koroteev, *et al.*, *Kvantovaya Elektron. (Moscow)* **10**, 1077 (1983) [*Sov. J. Quantum Electron.* **13**, 687 (1983)].

⁹O. A. Aktsipetrov and E. D. Mishina, *Dokl. Akad. Nauk SSSR* **274**, 62 (1984) [*Sov. Phys. Dokl.* **29**, 37 (1984)].

- ¹⁰H. W. Tom, T. F. Heinz, and Y. R. Shen, *Phys. Rev. Lett.* **51**, 1983 (1983).
- ¹¹N. Bloembergen, R. K. Chang, S. S. Jha, and C. H. Lee, *Phys. Rev.* **174**, 813 (1968).
- ¹²V. R. Novak and I. V. Myagkov, in: *Proc. Sixth All-Union Conf. on Charge Transfer Complexes and Ion-Radical Salts, Chernogolovka* (1984), p. 235.
- ¹³N. Bloembergen and P. S. Pershan, *Phys. Rev.* **128**, 606 (1962).
- ¹⁴V. R. Novak, I. V. Myagkov, and Yu. M. L'vov, in: *Proc. Thirteenth All-Union Conf. on Organic Semiconductors, Patent, Moscow* (1984), p. 192.
- ¹⁵H. Hamong, M. Vincent, and M. Dupeyrat, *Thin Solid Films* **60**, 21 (1980).
- ¹⁶F. G. Grunfeld and C. W. Pitt, *Thin Solid Films* **99**, 249 (1983).
- ¹⁷Y. Kogama, M. Yanagishita, S. Toda, and T. Matsuo, *J. Colloid and Interface Sci.* **61**, 438 (1977).
- ¹⁸P. A. Chollet and J. Messier, *Thin Solid Films* **99**, 197 (1983).
- ¹⁹D. Engelsens, *Surf. Sci.* **56**, 272 (1976).
- ²⁰C. W. Pitt and L. M. Walpita, *Thin Solid Films* **68**, 101 (1980).
- ²¹J. L. Oudar and J. Zyss, *Phys. Rev. A* **26**, 2016 (1982).
- ²²T. F. Heinz, H. W. K. Tom, and Y. R. Shen, in: *Surface Studies with Laser* (Aussenegg, ed.), Springer-Verlag, New York (1983).

Translated by A. Mason